

# Evolution of the surface sulfur composition of a Ru sulfide particle during CH<sub>3</sub>SH condensation reaction: sulfur migration from the bulk to the surface

Gilles Berhault and Michel Lacroix\*

Institut de Recherches sur la Catalyse, (CNRS UPR 5401) 2, Avenue Albert Einstein, 69626 Villeurbanne cedex, France. E-mail: [lacroix@catalyse.univ-lyon1.fr](mailto:lacroix@catalyse.univ-lyon1.fr); Fax: +33 (0)4 72 44 53 90

Received (in Strasbourg, France) 20th July 2000, Accepted 3rd November 2000

First published as an Advance Article on the web 4th January 2001

The condensation of methanethiol (CH<sub>3</sub>SH) into dimethylsulfide (CH<sub>3</sub>SCH<sub>3</sub>), which is a useful test reaction for probing the acid–base character of transition metal sulfide catalysts for carbon–heteroatom hydrogenolysis reactions, shows a systematic deactivation process at the beginning of the reaction before reaching steady-state activity. The solid surface of RuS<sub>2</sub> catalyst in equilibrium with the gas phase was examined by various techniques with the aim of understanding the mechanism responsible for this loss of activity, *e.g.* coke formation, poisoning by the reactant or the products, change in particle size, *etc.* X-Ray diffraction and elemental analysis showed neither the formation of carbonaceous deposits nor a sintering effect during the catalytic run. In contrast, a modification of the surface composition of the catalyst induced by the reaction was observed using temperature programmed reduction (TPR). This technique showed that large amounts of H<sub>2</sub>S are detectable after performing the catalytic test. Sulfur mass balance analyses demonstrate that these sulfur species are an integral part of the total sulfur content of the ruthenium sulfide particles. These surface modifications arise from sulfur migration from the bulk to the surface of the particles during reaction. Based on these experimental data and on a crystallographic model developed for RuS<sub>2</sub>, it is proposed that the methanethiol condensation reaction proceeds on monovacant Ru sites.

The industrial hydrotreating process is currently used in all refineries for cleaning up the various oil fractions by removing the S, N, O and the metals present in organic molecules. Depending on the nature of the heteroatom, hydrotreating refers to hydrosulfurization (HDS), hydrodenitrogenation (HDN), hydrodeoxygenation (HDO), and hydrodemetallation (HDM) reactions, which operate at temperatures ranging from 573 to 673 K and under several atmospheres of hydrogen.<sup>1</sup> Supported nanoparticles of transition metal sulfides are efficient systems for catalyzing all these reactions. Noble metal sulfides, namely RuS<sub>2</sub> and Rh<sub>2</sub>S<sub>3</sub>, are more active solids than MoS<sub>2</sub>-based industrial catalysts.<sup>2,3</sup> Fundamental work based on the determination of the catalytic properties of supported or bulk Mo or Ru sulfides has shown that a fully sulfided material is not active in catalysis and that sulfur vacancies must be created at the surface of the particle to provide catalytically active sites.<sup>4–6</sup> In a first approach, these results may be interpreted in terms of Sabatier's principle for which the metal–sulfur bond strength should be neither too weak nor too strong so that the surface can easily form and regenerate surface vacancies during the reaction cycle.<sup>7,8</sup> However, all the data were obtained using frozen states of reduced catalysts and testing their catalytic properties in model reactions such as the H<sub>2</sub>–D<sub>2</sub> isotopic exchange and olefin or diolefin hydrogenation. As these reactions proceed at temperatures lower than those required to adjust the catalyst composition upon hydrogen treatment, it was assumed that, in the absence of any sulfur atoms in the feed, the catalyst composition was not affected by the catalytic run.

The chemical properties of these vacant sites were recently characterized using the condensation of methanethiol (CH<sub>3</sub>SH or MeSH) into dimethyl sulfide (CH<sub>3</sub>SCH<sub>3</sub> or MeSM) as the model reaction.<sup>9</sup> IR spectroscopic studies of the interaction of MeSH with various reduced RuS<sub>2</sub> states have demonstrated

that this reactant dissociates upon chemisorption, leading to the formation of a proton and a thiolate-type moiety. The heterolytic character of the adsorption implies the presence of both a Lewis acidic site to fix the organic fragment and the presence of a basic sulfur center to trap the positively charged hydrogen species. The acidic character of the sulfur vacant sites was confirmed by pyridine chemisorption experiments and a nice correlation was obtained between the Lewis acid site density and the initial rate of the MeSH condensation reaction.<sup>10</sup> However, the evolution of the condensation rate *vs.* time on stream shows that the catalyst deactivates at the beginning of the reaction. In heterogeneous catalysis, catalyst deactivation often arises from coke deposition formed by oligo- or polymerization of unsaturated hydrocarbons at the surface of the particle.<sup>11</sup>

In our case this type of surface poisoning appears unlikely, taking into account the light molecules involved in the reaction and the relatively low reaction temperature (673 K). However, as sulfur-containing molecules are used in this model reaction, H<sub>2</sub>S chemisorption, resulfidation or solid reconstruction may modify the surface composition, leading to a diminution of the number of active sulfur vacant sites and therefore a decrease of the catalytic activity. The aim of this contribution is to discriminate between these various possibilities by controlling the sulfur-to-metal ratio of several reduced states of Ru sulfide. This could be achieved by measuring the sulfur mass balance during or at the end of the reaction using the temperature programmed reduction technique equipped with specific and sensitive detectors.

## Experimental

The catalyst was prepared by impregnation of a 300 m<sup>2</sup> g<sup>−1</sup> BET area silica (Grace Davison 432) with an aqueous solution

of  $\text{RuCl}_3 \cdot x\text{H}_2\text{O}$  (Johnson Matthey).<sup>9</sup> The impregnated silica was dried at 383 K and sulfided at 673 K in a 15%  $\text{H}_2\text{S}$ –85%  $\text{N}_2$  atmosphere in order to avoid the formation of an intermediate metallic phase that is difficult to sulfide.<sup>12</sup> After this activation procedure, the catalyst was cooled to room temperature under the sulfiding atmosphere, flushed with an oxygen-free nitrogen flow and stored in sealed bottles. The Ru loading was 7.5 wt.%.

Hydrogen reductive treatments and catalytic activity measurements were performed in the same flow microreactor connected to a gas chromatograph (HP 5890A) equipped with a flame photometric detector (FPD) and a flame ionization detector (FID) used, respectively, for the detection of  $\text{H}_2\text{S}$  and hydrocarbons. After loading the sample into the reactor, the solid was flushed under nitrogen for 15 min and then contacted with a hydrogen flow of  $100 \text{ cm}^3 \text{ min}^{-1}$  at room temperature. The reactor was then heated up to the desired reduction temperature ( $T_r$ ) using a heating rate of  $2 \text{ K min}^{-1}$  and left at this temperature for 2 h. The amount of  $\text{H}_2\text{S}$  released by the solid during the reduction process was quantified by calibrating the FPD detector with a known concentration of  $\text{H}_2\text{S}$  (1153 ppm) diluted in hydrogen.

After this *in situ* reduction step, hydrogen was replaced by nitrogen and the reactor temperature was fixed at 473 K. The reduced catalysts were then submitted to a flow containing 5.3 mol% of MeSH diluted in nitrogen. A HP-5 capillary column (crosslinked Ph-Me silicon,  $50 \text{ m} \times 0.32 \text{ mm} \times 0.25 \text{ }\mu\text{m}$ ) maintained at 333 K allowed the analysis of the reaction mixture. Besides the reactant (MeSH), only  $\text{H}_2\text{S}$  and dimethyl sulfide were detected under these experimental conditions. Conversions were kept lower than 10% by adjusting the total flow rate in order to avoid possible mass and heat transfer limitations.

X-ray diffraction measurements were performed to determine the structural stability as well as the modification of the particle size of the various reduced solids, either after reduction or after the solid had catalyzed the condensation reaction. XRD patterns were collected in the  $2\theta$  domain ranging from  $5$  to  $80^\circ$  using a Siemens D500 diffractometer together with a Cu- $\text{K}\alpha$  radiation source operating at 45 kV and 35 mA ( $\lambda = 1.5418 \text{ }\text{\AA}$ ). Particle size ( $\Phi$ ) was determined using the Scherrer equation:

$$\Phi = \frac{K \times \lambda \times 57.3}{\cos \theta \times \sqrt{\beta^2 - b^2}} \quad (1)$$

where  $\beta$  is the width at half-height of the experimental line.

The shape factor  $K$  was taken equal to 0.9 according to a previous electron microscopy study showing that the sulfided  $\text{RuS}_2$  particles are nearly spherical.<sup>13</sup> The correction factor  $b$  was determined using quartz powder as the internal standard ( $b = 0.11^\circ$ ). The reduced solids were transferred to the sample holder in a glove box and adhesive tape was used to protect them from air oxidation.

## Results

### Reduction and characterization of the catalysts

Elemental analysis indicates that the unreduced solid contains 6.4 wt.% of sulfur, which corresponds to an initial S : Ru ratio of 2.7. As reported in Table 1, this overstoichiometric sulfur is rather strongly bonded to the surface since its complete removal is observed only after heating the solid under hydrogen at 523 K while hydrogen treatment at 673 K is required to completely reduce the sulfided phase.

X-Ray diffraction patterns are reported in Fig. 1. The large peak centered at  $2\theta = 20^\circ$  and the shoulder at  $2\theta = 9^\circ$  are due to the silica support and the film used to protect the sample from air oxidation during the measurement. Besides these diffracting lines the unreduced solid presents three other peaks located at  $2\theta = 32, 46$  and  $54^\circ$ , respectively assigned to the [200], [220] and [311] faces of the  $\text{RuS}_2$  pyrite phase. A hydrogen treatment performed up to 573 K modifies neither the position nor the broadening of these diffraction lines. Thus the structure and the particle size of the solid (*ca.* 50  $\text{\AA}$ ) appear to be stable, in fairly good agreement with previously reported high resolution electron microscopy results<sup>9</sup> (see Table 1). At 623 K, the appearance of a new peak at  $2\theta = 43^\circ$ , corresponding to the [101] plane of the metallic phase, shows that the system becomes biphasic. At higher reduction temperatures, the diffraction lines of the sulfide phase disappear and only those corresponding to metallic Ru are detected at  $2\theta \approx 38.5$  [100],  $42.2$  [002],  $44.0$  [101],  $58.4$  [102] and  $69.5$  [110]. From these data, it is clear that the silica-supported ruthenium

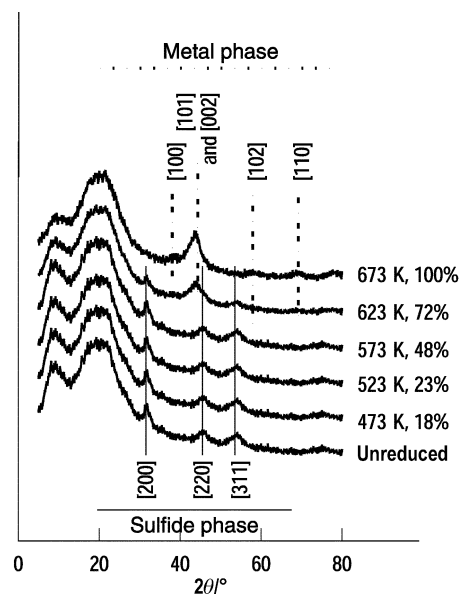


**Fig. 1** XRD patterns recorded for the catalyst reduced at various temperatures.

**Table 1** Degree of reduction and mean particle size after hydrogen treatment of  $\text{RuS}_2\text{-SiO}_2$  at various reduction temperatures ( $T_r$ ). Data in parentheses correspond to the standard deviation of the particle size distribution

$T_r/\text{K}$	Evolved $\text{H}_2\text{S}/\mu\text{mol g}^{-1}$	S : Ru	Mean particle size/ $\text{\AA}$	
			XRD	HREM <sup>9</sup>
None	None	2.7	52	36(7)
423	241	2.38	52	ND
473	400	2.16	54	37(8)
523	521	2	ND	ND
573	902	1.49	53	43(11)
623	1644	0.49	60	65(16)
673	2005	0	80–100	110(28)

sulfide maintains its morphology up to 573 K and when sintering occurs, the increase in the particle size is accompanied by the formation of a metallic phase. This is in agreement with the presence of only two phases, RuS<sub>2</sub> and metallic Ru, in the Ru–S phase diagram.

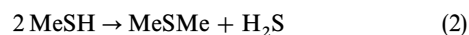
### Catalytic properties

Preliminary experiments have shown that the silica carrier, either sulfided or reduced at a temperature as high as 773 K, is not active in this reaction. Fig. 2 reports the evolution of the reactant conversion as a function of time on stream for the catalyst reduced at various temperatures. The NR curve refers to the activity of the unreduced solid. Its activity was determined after heating the catalyst up to the reaction temperature (473 K) in the presence of a nitrogen flow. During this step, the solid does not release any detectable amount of H<sub>2</sub>S, suggesting that its activity arises from the existence of sulfur vacant sites already present on the unreduced sample. Fig. 2 shows that the activity increases upon reduction up to  $T_r = 473$  K, and then declines for higher reduction temperatures. The activity enhancement could be ascribed to the creation of more numerous vacant sites accessible to the thiolate species formed by the heterolytic dissociation of MeSH. For higher degrees of reduction, the amount of sulfur atoms in the lattice decreases as well as the number of basic centers required for trapping the H<sup>+</sup> fragment. Therefore, the higher activity observed for  $T_r = 473$  K, leading to a degree of reduction close to 20%, corresponds to a maximum in the number of acid–base paired sites.<sup>9</sup> Besides this activity dependence towards solid reduction, Fig. 2 also shows distinct deactivation profiles. The unreduced catalyst as well as the solid reduced at 423, 623 and 673 K only exhibit a slight deactivation by comparison to the other samples for which the steady-state activity is about 25% lower than the initial activity. However, it should be noted that this deactivation does not modify the activity ranking against  $T_r$ . Accordingly, the diminution of catalyst activity should reflect a decrease in the number of active sites, leading to a lower number of sulfur vacancies per surface Ru cation.

### Origin of the deactivation

The main cause of deactivation in heterogeneous catalysis is due to sintering and/or coke formation. In our study, these hypotheses are unlikely to be due to the low temperature of reaction ( $T = 473$  K). This was confirmed by XRD profiles that do not differ before and after the CH<sub>3</sub>SH condensation reaction and by elemental analysis, which does not reveal the presence of carbonaceous deposits on the catalyst surface after reaction at 473 K. Consequently, both sintering and coke formation can be excluded as a source of deactivation. Another possible cause of catalyst deactivation would be to envisage

surface poisoning or catalyst resulfidation by the hydrogen sulfide formed in the reaction:



The poisoning effect of H<sub>2</sub>S when progressive amounts of this gas are added in the inlet feed<sup>1</sup> is a well-known phenomenon in hydrotreating catalysis. However, in such a situation, a difference between the MeSMe and the H<sub>2</sub>S outlet flows should be detected. Fig. 3 reports the flow difference *vs.* reaction time for the catalyst reduced at 573 K. Results evidence that only a slight deviation is observed since the integrated area underneath the curve represents only 20 μmol g<sup>−1</sup> of sulfur. Lower values were observed on the samples reduced at other temperatures. However, the possible resulfidation process could be slow enough so that sulfur balance deviation can not be detected.

In order to address this point, we have undertaken a set of consecutive temperature programmed reduction (TPR) experiments. The following methodology was used.

Step 1: the catalyst was reduced at  $T_r$  as described in the experimental section. The amount of sulfur eliminated during this step corresponds to the value reported in Table 1. Step 2: the temperature was lowered to the reaction temperature and the catalytic test was performed over 6 h. Some blank experiments were also carried out by replacing the reactant mixture with a pure nitrogen or hydrogen flow. Step 3: the reaction feed was replaced by a nitrogen flow for 15 min. During this step only a few ppm of MeSH and MeSMe were detected by online mass spectroscopy. An intermediate TPR was then performed by heating the solid from the reaction temperature (473 K) up to  $T_r$  in flowing hydrogen and remaining at this temperature until the complete disappearance of the H<sub>2</sub>S signal. Step 4: a third TPR was done by heating the catalyst from  $T_r$  to 773 K in order to completely transform the sulfided phase into the metallic one. A schematic depiction of these various steps is presented in Fig. 4 using as an example the data obtained for the solid reduced at 523 K.

The total sulfur content is obtained by adding the amount of sulfur liberated during the three consecutive TPRs. For the example illustrated in Fig. 4, this amount (2024 μmol g<sup>−1</sup>) is identical within the experimental error to that determined by chemical analysis (2005 μmol g<sup>−1</sup>). As reported in Table 2, similar results were observed irrespective of the degree of reduction resulting from step 1. These data indicate that the solid does not retain sulfur during the reaction course. Consequently, H<sub>2</sub>S poisoning and/or solid resulfiding do not explain the observed deactivation process. If the reduced catalysts are contacted with hydrogen or an inert gas during step 2, no H<sub>2</sub>S is released during the intermediate TPR (step 3), suggesting that an equilibrium between the gas phase and the solid is attained during the reduction step. In contrast, a significant amount of H<sub>2</sub>S is eliminated in step 3 if the various solids

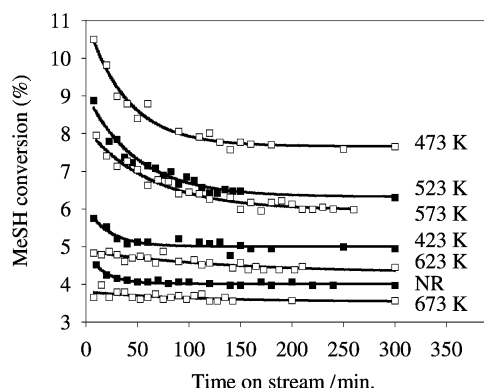


**Fig. 2** Evolution of the MeSH conversion as a function of time on stream for the catalyst reduced at various temperatures.

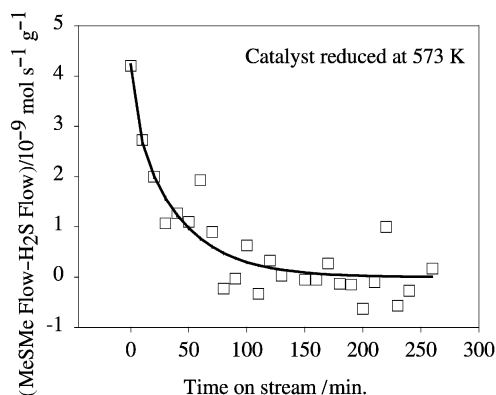


**Fig. 3** The flow difference between MeSMe and H<sub>2</sub>S *vs.* time on stream (initial state: solid reduced at 573 K).

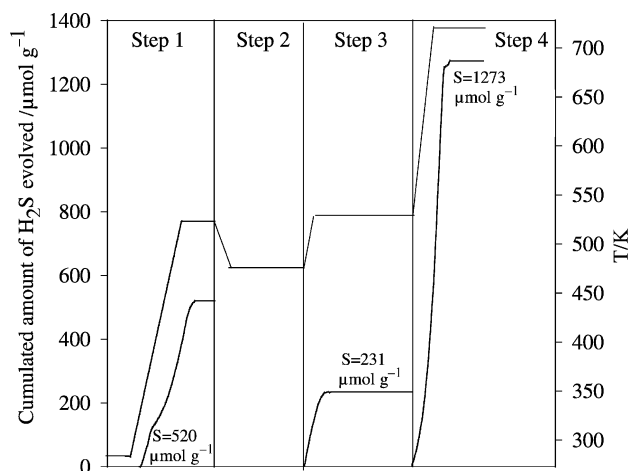


**Fig. 4** Schematic diagram representing the experimental procedure used for calculating the amount of sulfur migrating from the bulk to the surface of the catalyst. Step 1: reduction at 523 K; Step 2: reaction at 473 K; Step 3: TPR from 473 to 523 K; Step 4: TPR from 523 to 773 K.

have catalyzed the condensation reaction. As this amount does not alter the overall sulfur content, the composition of the surface was modified by sulfur migration from the bulk to the particle surface during the catalytic run.

## Discussion

The structure of  $\text{RuS}_2$  can be depicted as a modified NaCl structure with two interpenetrating fcc sublattices, one containing the Ru atoms and the other the S–S pairs.<sup>14</sup> Taking into account this crystal structure and the mean particle size determined by HREM, the fraction of the ruthenium and sulfur ions present at the surface of the supported nanoparticle can be evaluated using the crystallographic model proposed by Geantet *et al.*<sup>15–17</sup> According to this model, based on a three-dimensional growth of the fcc lattice of the  $\text{RuS}_2$  pyrite structure, the fraction of surface Ru cations represents 37% of the total Ru content. For this high surface-to-volume ratio, the ruthenium ions located at the corners and edges and those at the surface of the particle are sulfur deficient and may possess 3, 2 and 1 unsaturations, respectively. These coordinatively unsaturated sites might accommodate extra sulfur atoms to reach the six-fold coordination state during catalyst preparation, namely because of the rich sulfur atmosphere necessary to transform the supported Ru precursor into a sulfided state. From this model, a fully sulfided particle of 36 Å would lead to a S/Ru ratio of 2.9. This value is higher than the experimental S/Ru ratio determined by chemical analysis, suggesting that the unreduced catalysts might possess some vacant sulfur sites able to chemisorb electron-donating molecules such as MeSH and pyridine. Taking into account the sulfur content determined by chemical analysis as well as the

data calculated from the model, the estimated number of vacancies ( $V$ ) per superficial Ru ion ( $\text{Ru}_s$ ) is 0.54 [ $V/\text{Ru}_s = (2.9 - 2.7)/0.37$ ]. This proportion of anionic vacancies might reasonably explain the relatively high activity of the unreduced sample. As shown in Fig. 2, the deactivation of this catalyst is not really important, suggesting that the  $V/\text{Ru}_s$  ratio stays fairly constant during the reaction course.

The data reported in Fig. 2 also show that the most active catalyst was obtained after solid reduction at 473 K. At this temperature the composition of the sulfided phase corresponds to  $\text{RuS}_{2.16}$  and the  $V/\text{Ru}_s$  ratio attains 2 [ $V/\text{Ru}_s = (2.9 - 2.16)/0.37$ ] at the end of the reduction process. As the deactivation is marked, this  $V/\text{Ru}_s$  value should be corrected for the amount of migrating sulfur if we assume that the latter is the main cause of activity loss. Unfortunately, the amount of sulfur migration from the bulk to the surface is not known for this reduced sample since its determination requires a reduction temperature higher than that of the reaction temperature. However, Fig. 2 indicates that solids reduced at 473 and 523 K exhibit the same deactivation profiles, suggesting a rather similar amount of migrating sulfur. With this assumption, the corrected  $V/\text{Ru}_s$  ratio for the catalyst reduced at 473 K drops to 1.15, which is twice that over the unreduced sample. This relative proportion of vacant sites between both solids fits fairly well with their relative steady state activities since the activity of the solid reduced at 473 K is twice that of the unreduced solid.

## Conclusion

The present work gives the first experimental evidence of the migration of sulfur species from the bulk to the surface of small supported  $\text{RuS}_x$  particles. This process occurs when partially reduced states are contacted with sulfur organic substrates. The role of a reactant, the nature of the migrating species as well as the mechanism of this sulfur mobility are still unknown. It could be envisaged that during the approach of the acidic MeSH molecule a change in the surface potential may occur. This unstable surface intermediate state may then decrease its surface energy by reinforcing the population of sulfur basic centers, allowing for complete stabilization of the system by chemisorption of the reactant. Indeed, the augmentation of the concentration of sulfur surface atoms is a favorable process, which allows trapping of the proton formed by a heterolytic dissociation of MeSH. This emphasizes the difficulties of characterizing sulfided catalysts under working experimental conditions.

This study has shown that the Lewis acidic site required for the transformation of MeSH into MeSMe is likely a monovacant Ru site. With respect to spectroscopic techniques often used to characterize the interaction of probes with solid surfaces, the main advantage of utilizing a reaction is to identify the properties of solids under experimental conditions close to those used in the industrial hydrotreating applications of these sulfided materials.

## Acknowledgements

This work was carried out within the scope of a scientific program of collaboration between France and China (CNRS PICS No. 299). G. B. is greatly indebted to the French Ministry of Education for a Ph.D. grant.

## References

- 1 H. Topsøe, B. S. Clausen and F. E. Massoth, *Hydrotreating Catalysis—Catalysis Science and Technology*, Springer-Verlag, Berlin, 1996, vol. 11.
- 2 T. A. Pecoraro and R. R. Chianelli, *J. Catal.*, 1981, **67**, 430.
- 3 M. Lacroix, N. Boutarfa, C. Guillard, M. Vrinat and M. Breysse, *J. Catal.*, 1989, **120**, 473.

**Table 2** Amount of  $\text{H}_2\text{S}$  released during the consecutive TPR experiments

$T_r/\text{K}$	Evolved $\text{H}_2\text{S}/\mu\text{mol g}^{-1}$			Total S content $\mu\text{mol g}^{-1}$
	Step 1	Step 3	Step 4	
None	None	—	—	2005
523	521	231	1273	2024
573	902	464	658	2026
593	1186	348	486	2020
623	1644	246	139	2029
673	2005	None detectable	None detectable	2005

- 4 A. Tanaka, *Adv. Catal.*, 1985, **33**, 99.
- 5 A. Wambecke, L. Jalowiecki, S. Kasztelan, J. Grimblot and J. P. Bonnelle, *J. Catal.*, 1988, **109**, 320.
- 6 M. Lacroix, C. Mirodatos, M. Breyse, T. Décamp and S. Yuan, in *Proceedings of the 10th International Congress on Catalysis*, eds. L. Guzzi, F. Solymosi and P. Tétényi, Elsevier, Budapest, 1993, pp. 597–609.
- 7 H. Toulhoat, P. Raybaud, S. Kasztelan, G. Kresse and J. Hafner, *Prepr.-Am. Chem. Soc., Div. Pet. Chem.*, 1997, **42**, 114.
- 8 P. Raybaud, J. Hafner, G. Kresse and H. Toulhoat, *J. Phys.: Condens. Matter*, 1997, **9**, 11107.
- 9 G. Berhault, M. Lacroix, M. Breyse, F. Maugé, J.-C. Lavalley and L. Qu, *J. Catal.*, 1997, **170**, 37.
- 10 G. Berhault, F. Maugé, J.-C. Lavalley, M. Lacroix and M. Breyse, *J. Catal.*, 2000, **189**, 431.
- 11 E. Furimsky and F. E. Massoth, *Catal. Today*, 1999, **52**, 381.
- 12 O. Knop, *Can. J. Chem.*, 1963, **41**, 1838.
- 13 B. Moraweck, G. Bergeret, M. Cattenot, V. Kougionas, C. Geantet, J.-L. Portefaix, J. L. Zotin and M. Breyse, *J. Catal.*, 1997, **165**, 45.
- 14 O. Sutarno, O. Knop and I. G. Reid, *Can. J. Chem.*, 1967, **45**, 1391.
- 15 C. Geantet, C. Calais and M. Lacroix, *C. R. Séances Acad. Sci., Ser. II*, 1992, **315**, 439.
- 16 J. A. De Los Reyes, M. Vrinat, C. Geantet and M. Breyse, *Catal. Today*, 1991, **10**, 645.
- 17 C. Dumonteil, M. Lacroix, C. Geantet, H. Jobic and M. Breyse, *J. Catal.*, 1999, **187**, 464.